Biol Invasions (2024) 26:953–973
https://doi.org/10.1007/s10530-023-03222-0

ORIGINAL PAPER

Against the flow: Integrated taxonomy and environmental suitability of a cold-water species dispersing to warmer waters

Federica Montesanto · Racheli Hadjez · Francesco Mastrototaro · Dorothée Huchon · Carmela Gissi · Lion Novak · Noa Shenkar

Received: 19 February 2023 / Accepted: 30 October 2023 / Published online: 9 December 2023

Abstract The number of species dispersing to higher and/or lower latitudes, in association with temperature warming, is growing exponentially with only a few described opposite cases of dispersal to warmer regions. Here we describe the dispersal of the solitary ascidian *Ascidia virginea*, considered native to the seas of North Europe, to disperse to warmer regions: the Eastern Mediterranean and a Red Sea marina. This case highlights an emerging trend of taxa being introduced by marine vessels and successfully establishing populations in unfavourable environmental conditions by opportunistically utilizing niche areas. We provide molecular and morphological data that facilitate the identification of *A. virginea* in regions in which it may have previously been overlooked. We also employ ecological-niche modeling to project habitat suitability for this species, predicting the coasts of North America, South America, the northwest Pacific, and the Red Sea as moderately and highly suitable habitats. Phylogenetic analyses based on the mitochondrial COI gene reveal that the *A. virginea* sequences obtained in this work belong to a well-supported clade, including previously published sequences of *A. virginea* from California and Florida, localities where its presence was not predicted by our model. Furthermore, publicly available COI sequences of *A. malaca* and *A. sydneiensis* are

---

Supplementary Information The online version contains supplementary material available at https://doi.org/10.1007/s10530-023-03222-0.

F. Montesanto (✉)
University of Neberska–Lincoln, 3310 Holdrege Street,
Lincoln, NE 68583, USA
e-mail: fmontesanto@ufl.edu

F. Montesanto · F. Mastrototaro · C. Gissi
Department of Biosciences, Biotechnologies
and Environment, University of Bari "Aldo Moro", Bari,
Italy

F. Montesanto · F. Mastrototaro · C. Gissi
CoNISMa, Consorzio Nazionale Interuniversitario per le
Scienze del Mare, Rome, Italy

Present Address:
F. Montesanto
Whitney Laboratory for Marine Bioscience, University
of Florida, St. Augustine, FL, USA

R. Hadjez · D. Huchon · L. Novak · N. Shenkar (✉)
School of Zoology, George S. Wise Faculty of Life
Sciences, Tel-Aviv University, Tel Aviv, Israel
e-mail: shenkarn@tauex.tau.ac.il

D. Huchon · L. Novak · N. Shenkar
The Steinhardt Museum of Natural History and Israel
National Center for Biodiversity Studies, Tel-Aviv
University, Tel Aviv, Israel

C. Gissi
IBIOM, Institute of Biomembranes, Bioenergetics
and Molecular Biotechnologies, Consiglio Nazionale delle
Ricerche, Bari, Italy

assigned to the same *A. virginea* clade, implying a case of synonymy or misidentification. Our results provide useful data for the accurate identification of this species when expanding into other areas in which it may become a nuisance, and highlight the need to further explore the potential of cold-water species to establish in ports and niche areas in warmer regions.

Keywords Marine bioinvasions · Fouling · Shipping · Tunicata · Global warming · Ecological niche modeling · Maxent · COI · DNA barcoding

Introduction

While there are numerous cases of poleward shifts in species introductions in association with global warming, the opposite trend of dispersing to warmer regions, is relatively rare. However, in marine ecosystems there have been an increasing number of cases of species belonging to various taxa dispersing from higher and/or lower latitudes into warmer waters (Lima et al. 2007; Chang et al. 2020). Among invertebrates, for example, the copepods *Paracartia latisetosa* (Kriczaguin, 1873) and *Acartia (Acartiura) clausi* (Giesbrecht, 1889), the giant squid *Dosidicus gigas* (d'Orbigny, 1835), the sea slug *Chelidonura fulvipunctata* (Baba, 1938), the cushion star *Parvulastra exigua* (Lamarck, 1816), and the ascidians *Ciona robusta* (Hoshino & Tokioka, 1967) and *Corella inflata* (Huntsman, 1912), are currently being recorded in warmer regions than those previously known (Belmonte and Potenza 2001; Malaquias et al. 2016; Shenkar et al. 2017; Chang et al. 2020; Pinsky et al. 2020). In addition, various species of fish, including the spotted seabass *Dicentrarchus punctatus*, the meagre *Argyrosomus regius* (Asso, 1801), the golden grey mullet *Chelon auratus* (Risso, 1810), as well as the giant goby *Gobius cobitis* Pallas, 1814, and the rock goby *G. paganellus* Linnaeus, 1758, have been found to disperse into the northern part of the Red Sea from the Mediterranean Sea (Tiralongo et al. 2021).

A study evaluating the range shift of macroalgae along the Portuguese coast has shown that while warm-water species have expanded their range northwards, an analysis of cold-water species as a whole has revealed no significant trend of migration (Lima et al. 2007). This is primarily due to an equal number of cold-water species moving towards the north and towards the south, suggesting that these cold-water species may be resilient to changes in water temperature and other environmental factors. Recent studies further suggest that various assemblages of species may be moving in unpredicted directions (Nye et al. 2009; Pinsky et al. 2013), as well as individual taxa, such as the big skate *Raja binoculata* Girard, 1855 dispersing southward along the Pacific coasts of North America (Pinsky et al. 2013).

The use of Ecological-Niche Models (ENMs) has proven to be an effective approach for modeling the presence and distribution of many invasive species, particularly those in marine environments (Liu et al. 2011; Carlos-Júnior et al. 2015; Lins et al. 2018; Zhang et al. 2020). This is due to the ability of ENMs to integrate data on the environmental conditions suitable for the persistence of a species. Such data are crucial for understanding the factors that drive the expansion of invasive populations. ENMs conventionally predicate upon the notion that a species exhibits consistent environmental tolerance thresholds. However, recent empirical observations, as delineated in works by Nye et al. (2009) and Pinsky et al. (2013), underscore species colonizing regions beyond anticipated projections. These findings provide evidence for adaptive resilience and potential expanded tolerance parameters that were not historically accounted for. By characterizing the environmental conditions that promote the survival and persistence of invasive species, ENMs enable researchers to identify areas where such conditions are present and predict the potential range expansion of invasive populations (Melo-Merino et al. 2020). Indeed, ENMs present effective quantitative modeling approaches to understanding and predicting the range expansion of non-indigenous species (NIS), with the goal of identifying areas with suitable environmental conditions for NIS invasion compared to areas in which the same species is already known to be present (Franklin 2010). In order to understand and predict the range expansions of invasive species, it is necessary to characterize the current environmental conditions that are suitable for the persistence of a given species and identify the geographic areas where such conditions are present. ENMs offer a reliable tool for representing the predicted spatial response of a species to different environments (Pearson 2007; Cassini 2011), based on the assumption that the response functions estimated in ENMs accurately capture this relationship. Thus, ENMs provide an effective means of quantifying the risk or likelihood of ongoing or potential invasions, respectively, by integrating information about the current status of environmental conditions suitable for the persistence of a species (Locke and Hanson 2009). The findings should be however considered with caution as they do not incorporate population abundances (Peterson 2011; Owens et al. 2013; Januario et al. 2015).

Among marine taxa, the class Ascidiacea represents one of the worst "invaders", with frequent introductions into new regions via hull fouling (Rocha et al. 2015; Zhan et al. 2015; Gewing and Shenkar 2017; Lins et al. 2018; Zhang et al. 2020). The list of non-indigenous ascidian records has been constantly growing in the past decade, with new records of introductions worldwide (e.g., Rocha et al. 2019; Streit et al. 2021; Mastrototaro and Montesanto 2022; Mastrototaro et al. 2022; Nydam et al. 2022). These opportunistic species can tolerate a wide range of environmental parameters, which, combined with the lack of significant predators, results in their rapid growth and potential competition with the native species for food and space (Lambert 2007). The damage caused by these invasive ascidians results in increased management costs and antifouling treatments, as well as displacing and impacting commercial species (Adams et al. 2011; Aldred and Clare 2014; López-Legentil et al. 2015; Casso et al. 2018; Lins et al. 2018).

The focus of the current study, *Ascidia virginea* (Müller 1776), (Ascidiacea, Ascidiidae), is a solitary ascidian, also known as the "rectangular ascidian" due to the peculiar shape of its body. This species was first described from along the Norwegian coast by Müller (1776), who assigned it the specific name "*virginea*", referring to its smooth and whitish surface. The species is widely distributed along the coast of Northern Europe (northeastern Atlantic, Millar 1966; Brunetti and Mastrototaro 2017) and the western Mediterranean Sea (Brunetti and Mastrototaro 2017), and is commonly found on rocky substrates in sheltered or semi-exposed areas at 2–50 m depth (Millar 1966; Bay-Nouailhat and Bay-Nouailhat 2020).

Previous studies have shown that non-indigenous members of the Ascidiidae family are often detected in hull fouling and in marina species-community surveys (Skinner et al. 2016; Gewing and Shenkar 2017; Streit et al. 2021), highlighting the potential contribution of marine traffic to their dispersal and spread. Indeed, Chang et al. (2020) suggested that the range expansion of the cold-water ascidian *Corella inflata* to warmer-temperate latitudes along the California coastline can be linked to changes in vessel traffic patterns, which increase the likelihood of the introduction of fouling species. In addition, because the external appearance of the different Ascidiidae species is often similar, many misidentifications have occurred (e.g., Petović et al. 2018; Mastrototaro et al. 2019a, b, 2020a, b; Turon et al. 2020), further hindering our ability to detect any recent range expansions of a particular species.

Here we compared the morphology of specimens of *A. virginea* collected along the Israeli coastline with the available taxonomic descriptions of this species (Traustedt 1883 as *Phallusia venosa*; Berrill 1950; Millar 1966, 1970), as well as with taxonomic descriptions of all known species belonging to the genus *Ascidia* recorded to date for the eastern North Atlantic, in the Mediterranean basin, and in the Red Sea (Shenkar 2012; Brunetti and Mastrototaro 2017). In order to provide reliable data to facilitate its future identification, we employed an integrated approach comprising both morphological examination and the analysis of a long fragment of the mitochondrial COI sequence as a DNA barcode (Salonna et al. 2021). Furthermore, we constructed ecological niche models (ENMs) to predict habitat suitability for *A. virginea* under the present climatic scenario in the world's different coastal regions (according to Seebens et al. 2013), using species distribution data and marine predictor variables; and we evaluated the relative contribution of each predictor variable in order to identify the most critical ones.

Material and methods

Sampling and morphological analysis

Ca. 20 specimens were collected from the submerged surfaces of artificial structures (e.g., bridges, pontoons) in the Eilat marina (Red Sea, Israel), as well as from seven ports and marinas along the East-Mediterranean coast of Israel, at 1–2 m depth, from 2015 to 2022 (Fig. 1) (see Table S1 in Suppl. Materials for coordinates and descriptions for all locations).

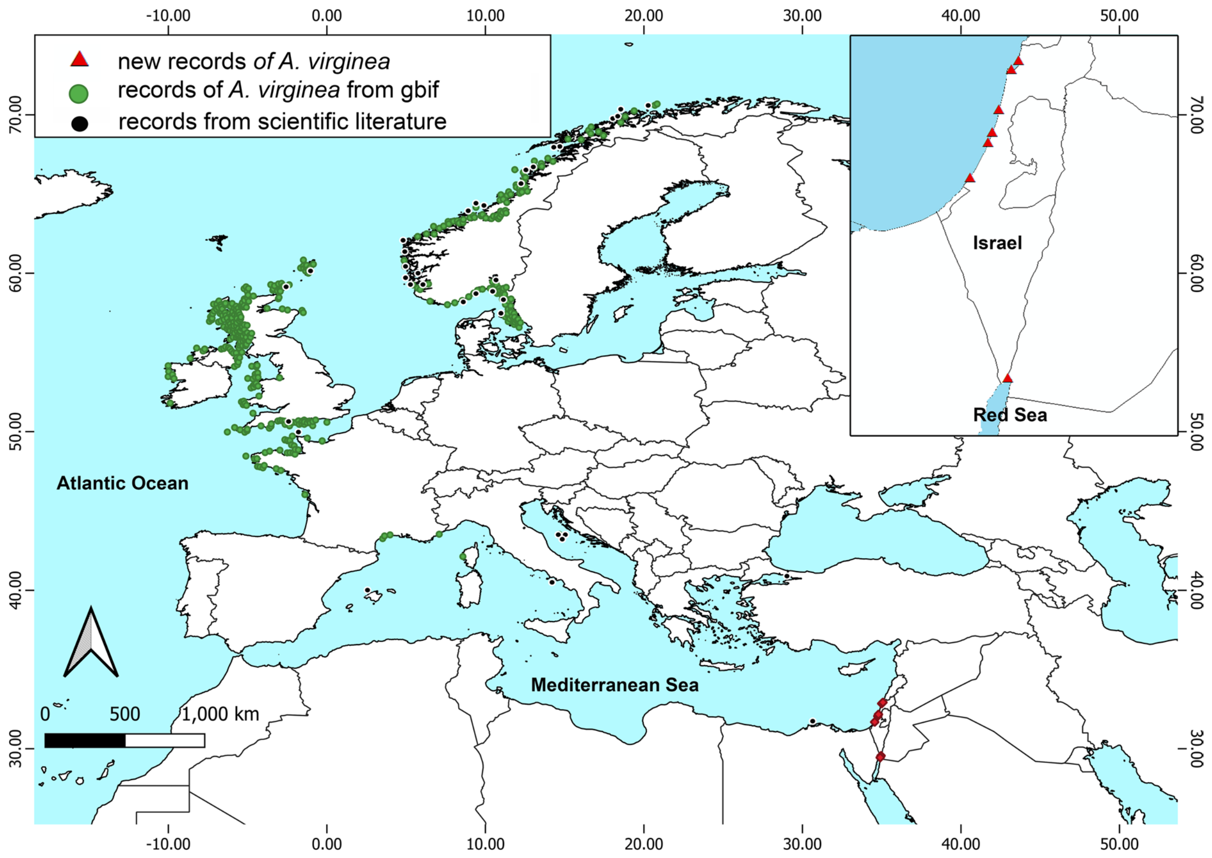

Fig. 1 Map of *Ascidia virginea* records extracted from the GBIF database and scientific literature (http://www.gbif.org, GBIF.org, accessed on 1st August 2022) after cleaning procedures (green dots) and records from the current study (red triangles)

For molecular analysis, 13 specimens (Table S1) were collected and directly preserved in 99% ethanol. For taxonomic identification, ca. 25 specimens were relaxed with menthol crystals for approximately three hours (until no contraction of the zooids was detected), and then preserved in a 4% formaldehyde solution in seawater. The latter specimens were morphological examined, dissected, and treated with Mayer's haemalum solution in order to identify their internal morphological characteristics, following Brunetti and Mastrototaro (2017).

Molecular analysis

Total DNA was extracted from the 13 individuals preserved in ethanol, following the protocol of Fulton et al. (1995). The extraction was performed on the dissected siphons. A fragment of the mitochondrial COI gene of ~ 850 bp was amplified with the primer pair dinF/Nux1R (Salonna et al. 2021). Because the yield of this first amplification was low, we used a nested-PCR strategy. Re-amplifications were performed using 1 µL of the first PCR products with the nested primers cat1F and ux1R (Salonna et al. 2021). All PCRs were performed with the Ex Taq polymerase (TaKaRa) in a 25 µl reaction volume containing: 1 µL of DNA template, 2.5 µL of 10X Ex Taq buffer, 0.2 µL of Ex Taq polymerase 5 µ/µL, 2 µL of dNTP mix 2.5 mM, 2 µL of each primer 5 mM, 0.5 µL of DMSO 100%, and 14.8 µL of ddH_2O. Amplification conditions were: (1) 4 min of initial long denaturation at 94 °C; followed by (2) 35 cycles of 30 s denaturation at 94 °C, 30 s of annealing at 50 °C, and 1 min of extension at 72 °C; and (3) a final elongation step for 5 min at 72 °C. The PCR products were cleaned from primer sequences by polyethylene glycol (PEG) precipitation using a 20% PEG, 2.5 M NaCl solution (Paithankar and Prasad 1991). The purified products were sequenced on an ABI 3500xl Genetic analyzer by the sequencing unit of the Life Sciences Faculty at Tel Aviv University, using the re-amplification primers. When needed, additional sequencing was performed using the internal primers "Fleb1F" (5′-TGT GGTTGGGAGTGGGGCAGGTAC-3′) and "Fleb1R" (5′-GTACCTGCCCCACTCCCAACCACA-3′). The 844 base-pair sequences are deposited in the European Nucleotide Archive under accession numbers OX416767–OX416775 and MW363030 (Table S1).

Phylogenetic and network analyses

Preliminary BLAST searches suggested that the obtained sequences belong to the suborder Phlebobranchia. To confirm the phylogenetic position of our sequences, a BLAST search limited to the taxon Phlebobranchia was conducted against the non-redundant nucleotide database (nr/nt) of the National Center for Biotechnology Information (NCBI) (November 21, 2022, www.ncbi.nlm.nih.gov/nuccore). A total of 808 sequences were downloaded. Of note, sequences that are labeled "Unverified" in the NCBI are excluded from the NCBI BLAST searches. Consequently, any such sequences present in the NCBI database were not included in our downstream analyses. The 808 sequences were aligned using the MAFFT v7.490 plugin (Katoh and Standley 2013) as implemented in Geneious Prime (2022.2.1 Biomatter Ltd), with the L-ins-i option and the codon translation option under the "Ascidian genetic code". Sequences presenting frame shifts were discarded. A preliminary tree was constructed with RaxML 8.2.11 (Stamatakis 2014) as implemented in Geneious Prime, using a Gamma Blossum62 protein model and the Rapid hill-climbing algorithm. This tree presented several sequences with long branches. BLASTx searches were conducted for each of these fast-evolving sequences, which enabled identification of putative taxonomically misidentified or misannotated sequences (detailed in Table S2). These sequences were removed, as well as all sequences shorter than 500 bp. When a species was represented by numerous closely-related haplotypes, four haplotypes representative of the species genetic diversity were selected manually and the others were discarded, except for sequences of the species *Ascidia virginea*, which were all retained. Members of the genus *Rhopalaea* were excluded since this genus belongs to the suborder Aplousobranchia (Shenkar et al. 2016). Finally, representatives of the genus *Ciona* were chosen as outgroup. The final dataset comprised 141 sequences, including the 9 sequences obtained in this work. The sequences were realigned based on codon translation as described above. Positions with more than 50% of missing data were excluded. We also observed that the start and end of several sequences were highly divergent and probably included sequencing errors, and therefore excluded these regions too from the alignment (Table S2). The final alignment comprised 804 positions.

Phylogenetic reconstructions were performed under the maximum likelihood and the Bayesian criteria with the programs IQ-Tree 1.6.12 (Nguyen et al. 2015) and MrBayes 3.2.7a (Ronquist et al. 2012) respectively. We first used Model Finder as implemented in IQ-Tree to determine the best model of evolution. The best fit model according to the Bayesian information criterion was a codon partition model with: position 1: GTR + F + I + G4; position 2: GTR + F + G4; and position 3: TPM2u + F + ASC + G4. Because the use of an ascertainment bias correction model (ASC) was not justified for the third codon position (ASC models are designed for datasets that intrinsically do not harbor constant sites) we used a GTR + F + G4 model for this position. The tree was reconstructed using an edge-linked-proportional partition model with separate models between partitions. Non-parametric bootstrap supports were computed based on 1000 replications. A Bayesian phylogenetic tree was reconstructed under the same partitioned model. The other parameters of the analyses comprised: two runs with four chains each, sampling every 100 generations, and a burnin fraction of 25%. The analyses were run for 10,000,000 generations. Before the burnin threshold was reached, we checked that the average standard deviation of split frequencies was below 0.01. Additionally, we verified at the end of the run that the Potential Scale Reduction Factor (PSRF) parameters were close to 1.0.

Based on the phylogenetic analyses, 28 sequences belonging to the *Ascidia virginea* clade were identified (see Results). A median-joining network (Bandelt et al. 1999) was reconstructed for these sequences using the program NETWORK v 10.0.0.0 (available at https://www.fluxus-engineering.com/sharenet.htm). Specifically, these COI sequences were realigned and alignment columns with missing data were removed. The alignment used in the network analyses comprised 28 sequences and 560 positions. The network was inferred under default parameters.

Ecological niche modeling (ENM)

Several studies have highlighted that the extent of the study area can influence the outcome of ENMs (VanDerWal et al. 2009; Barve et al. 2011; Lins et al. 2018; Zhang et al. 2020). Thus, since ascidians are mainly distributed in near-shore waters (Shenkar and Swalla 2011; Zhan et al. 2015), we considered only areas within the Exclusive Economic Zone (i.e., within 370 km of the coast). Georeferenced occurrence records of *A. virginea* were collected from the literature and from the Global Biodiversity Information Facility (http://www.gbif.org) (GBIF.org, accessed on 1st August 2022), along with our collected records (Fig. 1). It is important to note that this database cannot detect erroneous identifications on i-naturalist, scientific literature, and museum databases. Therefore, the exact source of each record is provided in Table S3, and future use of this data should be handled carefully. ArcGIS was used to check accuracy of all occurrence records prior to use. Records from GBIF.org with obvious geocoding errors were eliminated (such as the ones with coordinates corresponding to habitats not suitable for *A. virginea*, e.g., in the middle of the ocean), and very close and duplicate records from the same locality were removed manually. One occurrence per 5 arcminute grid cells (approximately 9.2 km by 9.2 km at the equator) was randomly selected (Lins et al. 2018; Zhang et al. 2020). Environmental suitability was modeled using variables from the Bio-Oracle dataset (http://www.bio-oracle.org) (Assis et al. 2018), which has 23 global marine environmental layers with a spatial resolution associated with a grid of cells of 5 arcminutes (approximately 9 km^2). Only variables that might limit ascidian distribution were selected and downloaded from this database, and water depth and distance to the shore were added (extracted from the Global Marine Environment Datasets, http://gmed.auckland.ac.nz) (Basher et al. 2014) to accurately reflect the known distribution patterns of ascidians as reported in similar studies (Lins et al. 2018; Zhang et al. 2020). Variables were checked for multicollinearity through a correlation matrix, randomly selecting only one among highly correlated variables (i.e., strongly correlated environmental variables with $|r| > 0.7$, Dormann et al. 2013). Based on correlation analyses and available empirical evidence, seven predictor variables (i.e., distance to shore, maximum values of chlorophyll A, minimum values of chlorophyll A, range values of temperature, mean values of temperature, range values of salinity, and mean values of salinity) were used to develop the ENMs.

The ENMs were fitted using Maximum Entropy Species Distribution Modeling software v.2.3 (Maxent). This is a valuable method for making predictions, particularly when information about species distribution is incomplete. By evaluating the climate data at each location where the species of interest is present, Maxent calculates a probability function that describes the chances of observing a species' presence given its observed distribution and the environmental conditions across the study area (Phillips et al. 2004, 2006; Januario et al. 2015). The output of Maxent provides a continuous variable that indicates environmental suitability. For each individual model, we used a 20-fold cross-validation scheme and randomly restricted 75% of the occurrence records for model training and 25% for testing the results, with 1,000 maximum iterations. The Area Under the Curve (AUC) statistic for the Receiver Operating Characteristic (ROC) was used to measure how well each model discriminates presence more accurately than a random prediction (Phillips et al. 2006). The AUC scores ranged from 0 to 1, with values < 0.5 indicating performance worse than random; a value of 0.5 indicating predictions no better than random discrimination; and a value of 1 representing perfect discrimination (Swets 1988). Fitted models, performed with occurrences records (namely "Europe and Red Sea"), were then projected over the different coastal regions across the world (according to Sebeens et al. 2013): "North America" (northeast and northwest Atlantic coastal regions); "South America" (southeast and southwest Atlantic coastal regions); and "Northwestern Pacific" (northwestern Pacific coastal region). It should be noted that coastal regions around Africa and Australia, as well as the northwestern Indo-Pacific region, were excluded from the modeling since a preliminary analysis did not reveal any areas suitable for *A. virginea*. The importance of each environmental variable for every model was assessed by a jackknife procedure, fitting models by using each variable separately and ranking them according to the test gain.

Results

Morphological analysis

Systematics

Phylum Chordata
 Subphylum Tunicata
 Class Ascidiacea
 Order Phlebobranchia
 Family Ascidiidae
 Genus *Ascidia*
 Ascidia virginea (Müller 1776)

New records

Red Sea coast of Israel: Eilat marina, submerged area of floating docks, 1–2 m depth, individuals from monitoring surveys carried out from 2015 to 2022 (Table S1 and Fig. 1).

Mediterranean coast of Israel: Akko, Haifa, Herzliyya, Jaffa, Ashqelon

Previous records

Mediterranean Sea: Pérès (1957), Heller (1875), Traustedt (1883), Ghobashy and Messeih (1991)

Aegean Sea: Koukouras et al. (1995)

Northwestern Atlantic Ocean: Arnbäck-Christie-Linde (1923), Berrill (1950), Millar (1966)

Arctic Ocean: Millar (1966)

Material examined

About 20 specimens from Eilat marina (Red Sea coast of Israel) (29°33′11.3″N, 34°57′35.9″E), and 5 specimens from Jaffa port (Mediterranean coast of Israel) (32°03′06.3″N, 34°44′58.1″E).

Five individuals preserved in 4% formalin with a tissue sample preserved in 99% ethanol are deposited in the collection of the Zoological Museum of the University of Bari (MUZAC-6669) and additional samples are deposited at the Steinhardt Museum of Natural History, Israel National Center for Biodiversity Studies, as detailed in Table S1 (AS26215F).

Morphological analyses

The specimens are about 4–5 cm in height with a thick semi-transparent tunic, gray or reddish in color (Fig. 2A), and were found attached to the substratum on the left side of their body. The atrial siphon is located at about 1/3 the length of the body. Both siphons have small-toothed lobes at their edges (Fig. 2A–D).

The oral siphon has numerous oral tentacles (about 50–60 long ones, alternated with smaller ones) and a pre-pharyngeal area finely papillated (Fig. 2E–F). The pharynx comprises 40–50 longitudinal vessels, with 4–5 stigmata per mesh (Fig. 2G), as measured in all examined individuals of the same size. Peculiar, small, three-lobed branchial papillae are located at the intersection between the transverse vessels, with short intermediate papillae visible between the branchial ones (Fig. 2H). The pharynx does not extend much beyond the stomach (Fig. 2K).

The dorsal tubercle is large, its aperture forms a U-shape with horns and is located close to the elongated neural ganglion (Fig. 2I). Below the dorsal tubercle, the dorsal lamina appears ribbed with a smooth edge (Fig. 2J).

The stomach is smooth, and the gut has both primary and secondary loop sharply bent and conspicuous (Fig. 2K). The position of the rectum is vertical, ending in a bilobed anus located close to the anterior limit of the gut loop (Fig. 2K). The gonads are located in the inner part of the intestinal loop, with the gonoducts opening close to the anus (Fig. 2K). A dark renal vesicle is sometimes present close to the stomach (Fig. 2B).

Remarks

Compared to the previous descriptions of *A. virginea* species made by Berrill (1950), Millar (1966, 1970), and Traustedt (as *Phallusia venosa* Traustedt 1883), we observed some differences in the specimens collected from the Eilat marina. In particular, the external appearance of our specimens (e.g., appearance of the tunic, shape/position of the siphons) does not fully match that of the previously described specimens of *A. virginea*, and some internal features also

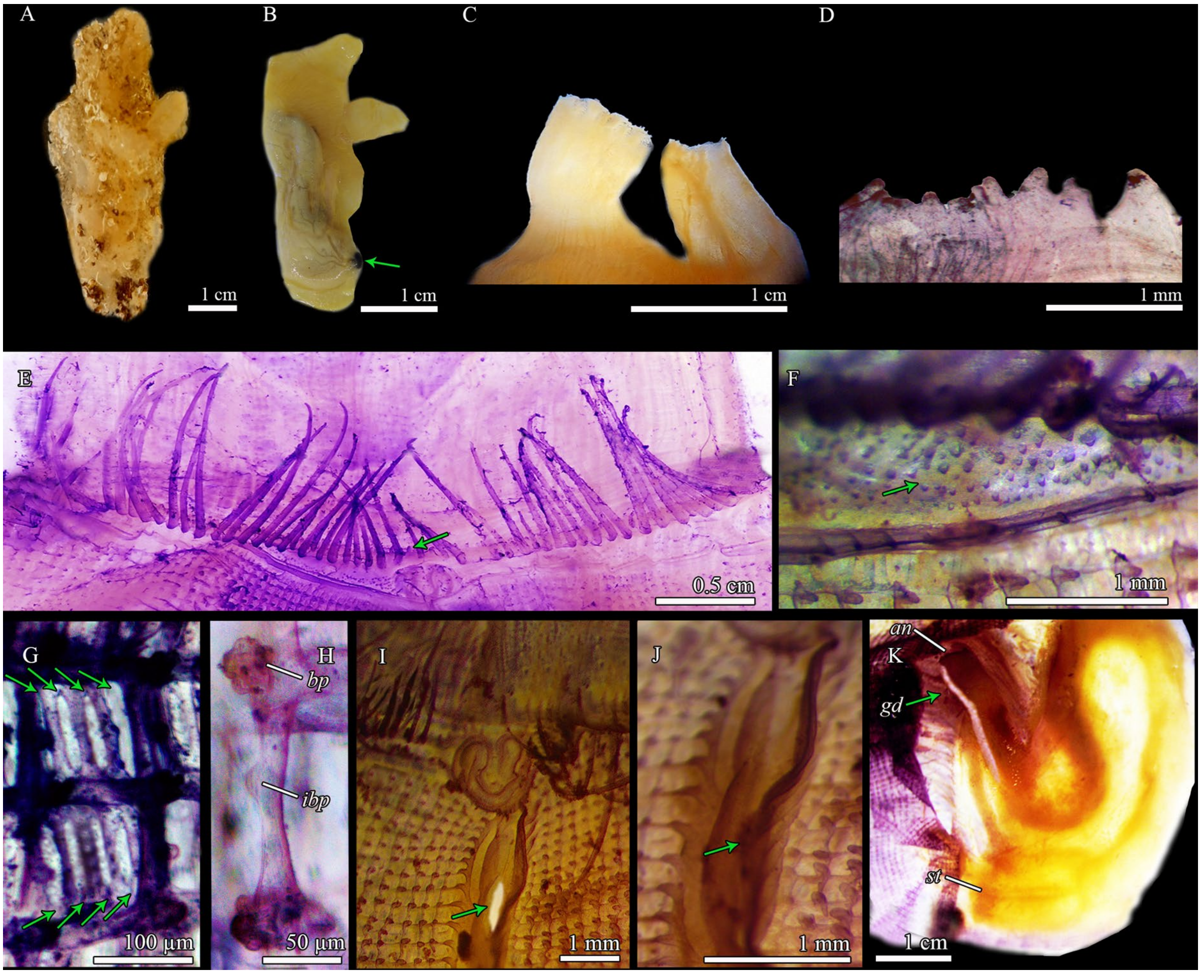

Fig. 2 *Ascidia virginea*. (**A**) Specimen with the tunic. (**B**) Specimen extracted from the tunic (arrow indicates a dark renal vesicle). (**C**) Oral and atrial siphon lying close to one another. (**D**) Magnification of the small-toothed lobes at the edge of the siphon. (**E**) Long thin oral tentacles alternating with shorter ones (indicated by the arrow). (**F**) Pre-pharyngeal area with papillae (arrow). (**G**) Magnification of the mesh of stigmata, with four stigmata per mesh (arrows). (**H**) Magnification of three-cornered branchial papillae (*bp*) and intermediate papillae (*ibp*). (**I**) Dorsal tubercle U-shaped with horns, located close to the neural ganglion (arrow). (**J**) Dorsal lamina ribbed (arrow) with smooth edge. (**K**) Alimentary canal with bent primary and secondary loop of the gut, smooth stomach (*st*), gonoducts (*gd*) opening (arrow) close to the bilobed anus (*an*)

show slight differences. Samples collected from Jaffa Port revealed similar distinguishing morphological characteristics to the samples from Eilat: pre-pharyngeal projections, three-lobed branchial papillae, and numerous long thin tentacles, but with a greater distance between the siphons (Figshare repository https://doi.org/https://doi.org/10.6084/m9.figshare.22589515).

Traustedt (1883, as *Phallusia venosa*) reported the presence of short siphons lying close to each other, a papillated pre-pharingeal area, the presence of branchial papillae, 6–8 stigmata per mesh, a dentated dorsal lamina, and the gut loop anterior to the anus.

Berrill (1950) also reported the presence of branchial papillae and smaller intermediate papillae. Furthermore, in his drawing it is possible to detect 4–5 stigmata per mesh. He also described a ribbed dorsal lamina without papillae, and either a wrinkled or smooth stomach followed by a gut with the secondary loop bent and close to the rectum, a character that Berrill considers as diagnostic of the species. The gonads are spread on the gut loop and the gonoducts

Table 1 Key to species of the genus *Ascidia* from European waters (modified after Brunetti and Mastrototaro 2017) and Red Sea

	1	2	3	4	5	6	7	8	9	10	11	12	13	14	15	16	17
Ascidia correi	T	At the posterior third of the body	Numerous long and thin	S	C	N	N	–	P	3–4	Initially double, simple before the ganglion, toothed edge, ribbed on the left and papillated on the right	–	–	Smooth anus, S	Large, white, around stomach	O	N
Ascidia molguloides	C	At 2/3 the body length	25 thin, 3 orders	S	Simple fissure	N	–	About 30	–	1–2	Initially double until the ganglion, smooth edged, ribbed	F	H	Slightly P	Small	–	N
Ascidia tritonis	–	At 1/2 or 1/3 the body length	Numerous long and thin, equal size	S	H	N	B	100 on each side, thin	A	3–4	Toothed	–	H	Very P	Few	–	F
Ascidia obliqua	–	At 1/2 or 1/3 the body length	About 70	S	U	N	–	–	A	–	R, with smooth edge or with small teeth	F	–	P	–	–	N
Ascidia prunum	–	Near-by (oral 8 lobes, atrial 6 lobes)	40–50	–	U	N	N	40–70	P	about 5	R	–	O–V	P	–	–	N
Ascidia malaca	wrinkled	Very long oral siphon, atrial siphon halfway	About 60 of various orders	S	H	F	B	–	–	6–8	S with toothed edge	/	V	Bilobed, slightly P	–	–	N
Ascidia celtica	–	At 1/3 body length	25 long	S	–	F	B	–	P	–	Initially double than ribbed and toothed	–	O	Slightly A	Large, numerous, covering gl and gonads	–	–
Ascidia muricata	P	At 2/3 the body length	40–60	S	–	F	B	40–50	P	4–7	L	–	H	smooth or bilobed anus, P	–	–	N

Table 1 (continued)

	1	2	3	4	5	6	7	8	9	10	11	12	13	14	15	16	17
Ascidia mentula	T	At the middle of the body	Up to 100 alternating in size	S	H	F	–	–	–	–	S with marginal teeth	–	H	–	Yellowish	–	N
Ascidia conchilega	C	At 1/3 body length	Thin, 40–120, 3 rows	S	H	1/6 of body lenght from dorsal tubercle	Slightly B	–	P	–	–	F	H	A	Large, dark, covering gl and gonads	O	–
Ascidia salvatoris	P	At 2/3 the body length	50–60 of 3–4 orders	P	H	F	B	–	P	–	Forming long languets at the edge, with 1–2 teeth between them	–	H	smooth anus, very P	–	–	N
Ascidia colleta	P	–	Irregular 30 long thin	P	–	F	Slightly B	60, no parastigmatic vessels	P	7–9	initially double than ribbed and toothed and with some papillae	S	H	Bilobed anus, A	Large, whitish	–	–
Ascidia interrupta	P	Halfway the body	100 or more, regular long and thin	P	H	F	B	–	A	6–9	S, only small lobes, no papillae	–	O	P	Few, small, sometimes absent	–	N
Ascidia iberica	T	Both 7 lobed, atrial siphon halfway	70, 3 orders	–	U	Halfway between the siphons	B	About 100 sometimes interrupted	A	–	–	–	V	Lobed anus slightly P	Transparent around intestine	–	N
Ascidia involuta	coated	Halfway the body	60	P	C	N	B	More than 100	_	4–6	Initially double, simple after the ganglion	S	H	_	Small	–	F
Ascidia dijmphiana	T	N	–	S	–	N	N	50–70	P	3–4	R with toothed edge	F	V	A	–	–	N
Ascidia savignyi	T	N	About 60		–	N	B	48–64 (R),39–52 (L)	P	5–6	S with small teeth	–	V	Bilobed anus, P	–	I	/

Table 1 (continued)

	1	2	3	4	5	6	7	8	9	10	11	12	13	14	15	16	17
Ascidia mediterranea	T	At 1/3 the body length	From 20 to 26, 3 orders	S	H	N	B	–	–	–	Initially S then with languets, no papillae	–	V	P or S	–	–	N
Ascidia callosa	P	N	Up to 30	S–P	C	–	N	<20	P	10 or more	–	–	V	Slightly A	Large, numerous, covering gl and gonads	–	N
Ascidia sulcata	T	–	Irregular long, 60 or more	–	U	N	–	–	–	–	–	–	–	Bilobed or smooth anus, P	–	–	–
Ascidia virginea	T	Scarcely evident, N	100 or more	P	–	N	N	About 50 (R), 40 (L) in individual of about 4 cm	P	6–8	S with small teeth, papillae on right side	Partially F or S	V	bilobed anus A or S	present	I	N
Ascidia virginea **(current study)**	**T**	**N**	**50–60 long, alternated with small ones**	S	**U**	**N**	Slightly B	**About 50 (R), 40 (L) in individual of about 4 cm**	**P**	4–5	**S with toothed edge**	**S**	**V**	**Bilobed anus, A or S**	**Present, dark**	**I**	**N**

(1) *Tunic*: T = thin, transparent, S = semi-transparent, thick, P = with small papillae, C = coated. (2) *Position of the siphons*: N = near-by. (3) Number of oral tentacles. (4) *Edge of dorsal lamina*: S = smooth, T = toothed or with languets. (5) *Dorsal tubercle*: H = horse-shoe shaped, U = U-shaped with horns, C = C-shaped. (6) *Position neural ganglion*: N = near dorsal tubercle, F = far from dorsal tubercle. (7) *Branchial sac*: N = not extending beyond the stomach, B = extending beyond the stomach. (8) Number longitudinal vessels on right (R) and left (L) side of the branchial sac. (9) *Intermediate papillae*: A = absent, P = present. (10) Number of stigmata per mesh. (11) *Dorsal lamina*: S = smooth, R = ribbed, L = with languets. (12) *Stomach*: S = smooth, P = partially folded. (13) *Rectum*: V = vertical, H = horizontal, O = oblique. (14) *Position of the anus*: P = posterior to the anterior edge of the gut loop, A = anterior to the anterior edge of the gut loop, S = same level of the anterior edge of the gut loop. (15) *Renal vesicles*: P = present (gl gut loop). (16) *Gonads*: I = inner part of the gut loop, O = on the gut loop. (17) *Gonoducts opening*: N = near the anus, F = far from the anus

Bold: morphological characters of the Eilat specimens in agreement with previous *A. virginea* descriptions end close to the bilobed anus, with the presence of renal vesicles.

Regarding the branchial papillae, Pérès (1957) reported the presence of intermediate papillae in the pharynx but did not refer to the trifurcate shape of the branchial ones, while Salfi (1931) did not observe the presence of intermediate branchial papillae. A drawing from Salfi's work (1931) illustrates the pharynx with 5–6 stigmata per mesh. Finally, Traustedt (1883), describing *Phallusia venosa*, subsequently synonymized with *A. virginea* (see Brunetti and Mastrototaro 2017), reported the presence of papillae in the pre-pharyngeal area, a pharynx with 60–70 oral tentacles of different orders, generally 6–8 stigmata per mesh, and ribbed dorsal lamina; but he did not refer to the presence of intermediate branchial papillae.

Berrill (1950) reported 60–120 tentacles of different sizes, with the largest of them being about 40 in number.

Finally, Millar (1966, 1970) in his key to species distinguished *A. virginea* in the position of the dorsal tubercle (close to the neural ganglion), the presence of about 40 longitudinal vessels on each side of the pharynx, and the thick cartilaginous tunic. Furthermore, he described specimens as red or gray in color, with about 100 oral tentacles, the anus placed anterior or close to the anterior limit of the gut loop, and the right side of the dorsal lamina papillated. Table 1 provides a comparison of our specimens with taxonomic descriptions for all known species belonging to the genus *Ascidia* recorded to date from the eastern North Atlantic, the Mediterranean basin, and the Red Sea (Shenkar 2012; Brunetti and Mastrototaro 2017).

To date, 21 species of the genus *Ascidia* Linnaeus, 1767 have been recorded in European waters and the Red Sea (Shenkar 2012; Brunetti and Mastrototaro 2017). Among these species, only five have their siphons arranged close to each other: *A. callosa* (Stimpson, 1852), *A. mediterranea* (Pérès, 1959), *A. dijmphniana* (Traustedt, 1886), *A. virginea* (Müller 1776), and *A. sulcata* (Savignyi, 1816) (Table 1).

A. callosa has a pharynx with only 20 longitudinal vessels, but more than 10 stigmata per mesh, while *A. mediterranea* has only 20–26 oral tentacles and a smooth pre-pharyngeal area. Both *A. dijmphniana* and *A. sulcata* are characterized by a thin, transparent, and glossy tunic. *A. dijmphniana* has a 7-lobed oral siphon and a 6-lobed atrial one with a smooth pre-pharyngeal area. *A. sulcata* is also characterized by peculiar deep longitudinal furrows and irregularly arranged oral tentacles (Brunetti and Mastrototaro 2017).

Among the species belonging to the genus *Ascidia*, only *A. sulcata,* and *A. savignyi* (Hartmeyer, 1915) have been reported to date from the Red to Sea (Shenkar 2012). *A. savignyi* is endemic to the Red Sea (Shenkar 2012), and was described by Hartmeyer in 1915, who reported the main difference between *A. savignyi* and *A. virginea* as being their different number of longitudinal vessels (higher in *A. savignyi*), as observed in specimens of similar size.

In conclusion, although there are some inconsistencies between the morphological features of the examined specimens from the coasts of Israel compared to previous descriptions of *A. virginea*, these differences mainly concern the shape/position of the siphons and the absence of papillae on the dorsal lamina (Table 1). This latter characteristic was not reported by all authors (Berrill 1950; Millar 1966, 1970; Traustedt 1883), which further questions its validity as a distinguishing feature. The identified inconsistencies could also be related to morphological differences between distant populations. We report several morphological characters of the examined material from the Eilat and the Mediterranean specimens that well agree with those reported in the previous descriptions of *A. virginea*, as follows: short siphons positioned close to each other (even though this characteristic is more evident for the Red Sea specimens), papillated pre-pharyngeal area, bilobed anus at the same level as the anterior edge of the gut loop, the bottom position and the sharp loops of the gut, long rectum, the gonoducts opening near the anus, pharynx with 40–50 longitudinal vessels, the presence of branchial intermediate papillae, and the pharynx not extending much beyond the stomach (see bold in Table 1). Finally, the difference in the number of tentacles compared to those reported by Millar (1966, 1970) can be explained as a consequence of our reporting only the number of the longest ones.

Phylogenetic analysis

The phylogenetic tree places, with high support (ML bootstrap support, BS = 99; Bayesian posterior probabilies, PP = 1.0), the sequences obtained in this work in a clade that contains sequences from

Ascidia virginea from Spain (López-Legentil et al. 2015) and Norway (Nydam and Lambert, unpublished), as well as from California (Nichols et al. 2023), Florida (Nydam, unpublished), and the Andaman and Nicobar Islands (northeastern Indian Ocean) (Ananthan and Murugan 2018) (Fig. 3A). This clade also includes sequences from two other species: *A. sydneiensis* (from Puerto Rico, Streit et al. 2021) and *A. malaca* (from Italy, Virgili et al. 2022). After trimming all sequences to the same length (560 basepairs), pairs of sequences within this clade showed up to 10 differences (i.e., less than 2% divergence), except sequence KJ725162 (Ananthan and Murugan 2018) from the Andaman and Nicobar Islands, which showed 25–33 base differences (i.e., 4.5–5.9% divergence) from the other sequences (see also the longest branch of KJ725162 in Fig. 3B). Of note, these 25 substitutions are all synonymous substitutions when compared to the major *A. virginea* haplotype, and they result in the same amino acid sequence. As it is annotated as *A. virginea* and its removal did affect the network topology for the rest of the sequences we included it in the current analysis. The median-joining network reveals that the Mediterranean Sea region to be the most diverse, with five different haplotypes; while three haplotypes were found in the northwest Atlantic. Remarkably, one haplotype was found in all regions.

Ecological-niche modeling

The test and training AUC values obtained for all the performed models were high, ranging from 0.9781 to 0.9818 (Table S4). The evaluation of the variable contributions, supported by jackknife analyses, implied that “land distance”, “temperature mean”, and “chlorophyll min” had the highest explanatory power, and thus were identified as the three most important variables (Table S4), followed by “chlorophyll max”, “temperature range”, and “salinity mean”. The performed models highlighted a widespread potential distribution of *A. virginea* in the northern Europe seas, Northwest Atlantic, Northeast Pacific, southernmost coasts of Argentina and Chile, and the Eastern Asiatic coasts (Fig. 4).

The model performed for “Europe and the Red Sea” adequately covers the native range of *A. virginea* and suggests that the most suitable habitat areas for this species (indicated by the high habitat suitability values) are along the Northern-Europe coasts, including Iceland (Fig. 4A).

In the eastern Mediterranean Sea *A. virginea* has already spread along the Israeli coasts and has also been reported from along the Egyptian coasts (Ghobashy and Messeih 1991), which the model displays as adequately suitable (Fig. 4B). Additional areas along the Turkish and Egyptian coasts also showed moderate suitability habitat values for *A. virginea* (Fig. 4A–B). Although the fewer occurrences of this species in warmer areas (e.g., southeastern Mediterranean Sea and the Red Sea) may have influenced the habitat suitability results, these areas were nonetheless identified as moderately suitable habitats in the performed ENMs. Other potentially suitable regions currently lacking the presence of *A. virginea*, as highlighted in the projected models (i.e., “North America”, “South America”, and “Northwest Pacific”), comprise extensive areas along the western and eastern coasts of Canada, as well as the southern coasts of Argentina and Chile, all of which showed high habitat suitability values for *A. virginea* (Fig. 4C–D); as did also for the northwest Pacific coasts (Fig. 4E).

Discussion

In this study we update the distribution map of the solitary ascidian species *Ascidia virginea* in the eastern Mediterranean Sea and the Red Sea. Native to Northern Europe (Nichols et al. 2023), this species should be considered as "non-indigenous" in the Red Sea, and in particular, as “established” in the Eilat marina due to the discovery of numerous reproductive individuals extensively colonizing the artificial substrata in this area during systematic monitoring and sampling efforts carried out since 2015 (Shenkar unpublished data). In the Levant Basin, its current restricted distribution in ports and marinas, the lack of established communities on natural substrates, and its historical absence from various inventory lists, further support its status as a non-indigenous species to the region.

Non-indigenous species of ascidians are more likely to be found in harbors, which represent well-known gateways for species’ introductions (Stachowicz et al. 2002; Simkanin et al. 2012; Airoldi et al. 2015; López-Legentil et al. 2015; Nichols et al. 2023), and where eutrophication (nutrient enrichment

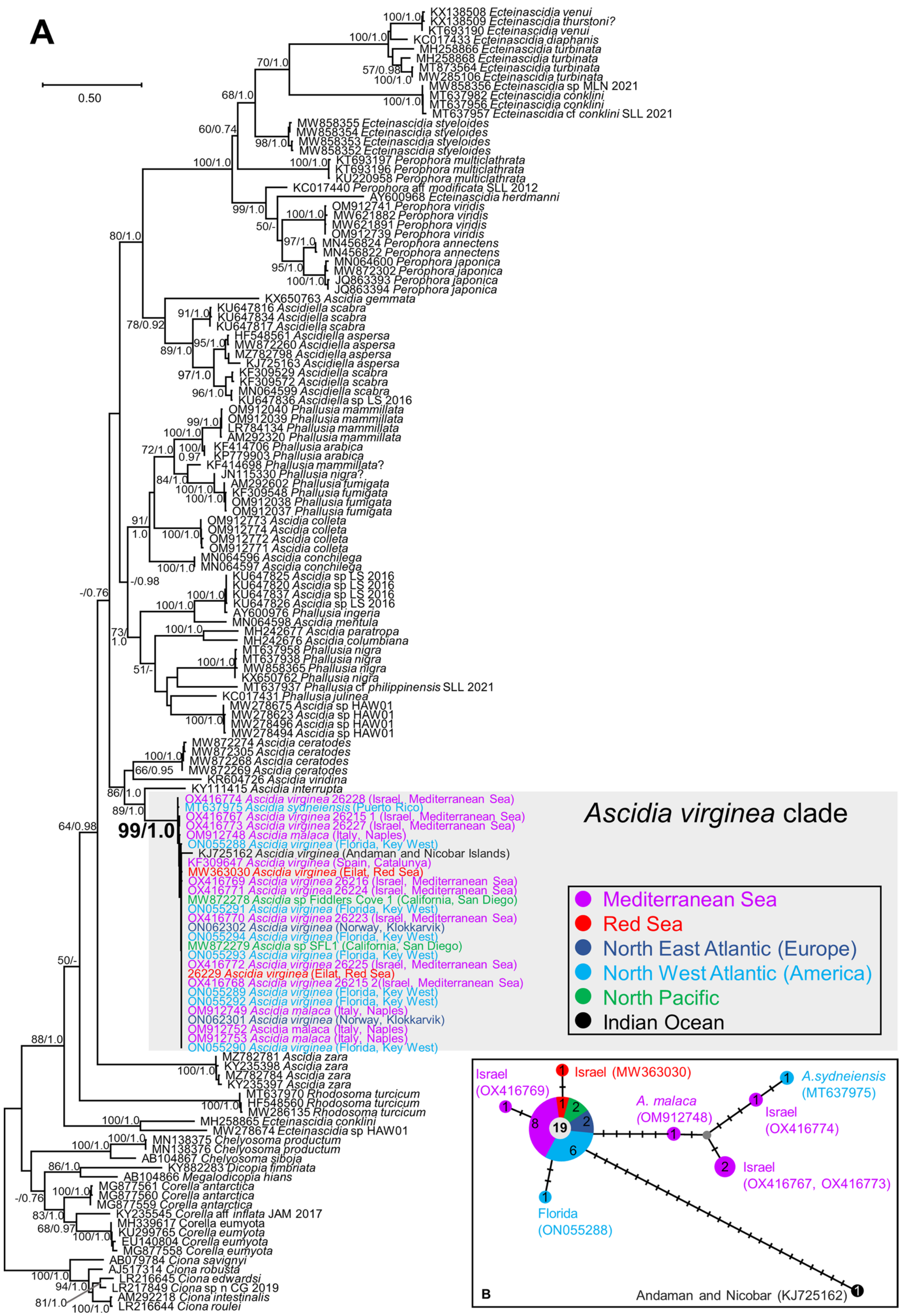
A
0.50
KX138508 Ecteinascidia venui
KX138509 Ecteinascidia thurstoni?
KT693190 Ecteinascidia venui
KC017433 Ecteinascidia diaphanis
MH258866 Ecteinascidia turbinata
MH258868 Ecteinascidia turbinata
MT873564 Ecteinascidia turbinata
MW285106 Ecteinascidia turbinata
MW858356 Ecteinascidia sp MLN 2021
MT637982 Ecteinascidia conklini
MT637956 Ecteinascidia conklini
MT637957 Ecteinascidia cf conklini SLL 2021
MW858355 Ecteinascidia styeloides
MW858354 Ecteinascidia styeloides
MW858353 Ecteinascidia styeloides
MW858352 Ecteinascidia styeloides
KT693197 Perophora multiclathrata
KT693196 Perophora multiclathrata
KU220958 Perophora multiclathrata
KC017440 Perophora aff modificata SLL 2012
AY600968 Ecteinascidia herdmanni
OM912741 Perophora viridis
MW621882 Perophora viridis
MW621891 Perophora viridis
OM912739 Perophora viridis
MN456824 Perophora annectens
MN456822 Perophora annectens
MN064600 Perophora japonica
MW872302 Perophora japonica
JQ863393 Perophora japonica
JQ863394 Perophora japonica
KX650763 Ascidia gemmata
KU647816 Ascidiella scabra
KU647834 Ascidiella scabra
KU647817 Ascidiella scabra
HF548561 Ascidiella aspersa
MW872260 Ascidiella aspersa
MZ782798 Ascidiella aspersa
KJ725163 Ascidiella aspersa
KF309529 Ascidiella scabra
KF309572 Ascidiella scabra
MN064599 Ascidiella scabra
KU647836 Ascidiella sp LS 2016
OM912040 Phallusia mammillata
OM912039 Phallusia mammillata
LR784134 Phallusia mammillata
AM292320 Phallusia mammillata
KF414706 Phallusia arabica
KP779903 Phallusia arabica
KF414698 Phallusia mammillata?
JN115330 Phallusia nigra?
AM292602 Phallusia fumigata
KF309548 Phallusia fumigata
OM912038 Phallusia fumigata
OM912037 Phallusia fumigata
OM912773 Ascidia colleta
OM912774 Ascidia colleta
OM912772 Ascidia colleta
OM912771 Ascidia colleta
MN064596 Ascidia conchilega
MN064597 Ascidia conchilega
KU647825 Ascidia sp LS 2016
KU647820 Ascidia sp LS 2016
KU647837 Ascidia sp LS 2016
KU647826 Ascidia sp LS 2016
AY600976 Phallusia ingeria
MN064598 Ascidia mentula
MH242677 Ascidia paratropa
MH242676 Ascidia columbiana
MT637958 Phallusia nigra
MT637938 Phallusia nigra
MW858365 Phallusia nigra
KX650762 Phallusia nigra
MT637937 Phallusia cf philippinensis SLL 2021
KC017431 Phallusia julinea
MW278675 Ascidia sp HAW01
MW278623 Ascidia sp HAW01
MW278496 Ascidia sp HAW01
MW278494 Ascidia sp HAW01
MW872274 Ascidia ceratodes
MW872305 Ascidia ceratodes
MW872268 Ascidia ceratodes
MW872269 Ascidia ceratodes
KR604726 Ascidia viridina
KY111415 Ascidia interrupta
OX416774 Ascidia virginea 26228 (Israel, Mediterranean Sea)
MT637975 Ascidia sydneiensis (Puerto Rico)
OX416767 Ascidia virginea 26215 1 (Israel, Mediterranean Sea)
OX416773 Ascidia virginea 26227 (Israel, Mediterranean Sea)
OM912748 Ascidia malaca (Italy, Naples)
ON055288 Ascidia virginea (Florida, Key West)
KJ725162 Ascidia virginea (Andaman and Nicobar Islands)
KF309647 Ascidia virginea (Spain, Catalunya)
MW363030 Ascidia virginea (Eilat, Red Sea)
OX416769 Ascidia virginea 26216 (Israel, Mediterranean Sea)
OX416771 Ascidia virginea 26224 (Israel, Mediterranean Sea)
MW872278 Ascidia sp Fiddlers Cove 1 (California, San Diego)
ON055291 Ascidia virginea (Florida, Key West)
OX416770 Ascidia virginea 26223 (Israel, Mediterranean Sea)
ON062302 Ascidia virginea (Norway, Klokkarvik)
ON055294 Ascidia virginea (Florida, Key West)
MW872279 Ascidia sp SFL1 (California, San Diego)
ON055293 Ascidia virginea (Florida, Key West)
OX416772 Ascidia virginea 26225 (Israel, Mediterranean Sea)
26229 Ascidia virginea (Eilat, Red Sea)
OX416768 Ascidia virginea 26215 2(Israel, Mediterranean Sea)
ON055289 Ascidia virginea (Florida, Key West)
ON055292 Ascidia virginea (Florida, Key West)
OM912749 Ascidia malaca (Italy, Naples)
ON062301 Ascidia virginea (Norway, Klokkarvik)
OM912752 Ascidia malaca (Italy, Naples)
OM912753 Ascidia malaca (Italy, Naples)
ON055290 Ascidia virginea (Florida, Key West)
Ascidia virginea clade
99/1.0
● Mediterranean Sea
● Red Sea
● North East Atlantic (Europe)
● North West Atlantic (America)
● North Pacific
● Indian Ocean
MZ782781 Ascidia zara
KY235398 Ascidia zara
MZ782784 Ascidia zara
KY235397 Ascidia zara
MT637970 Rhodosoma turcicum
HF548560 Rhodosoma turcicum
MW286135 Rhodosoma turcicum
MH258865 Ecteinascidia conklini
MW278674 Ecteinascidia sp HAW01
MN138375 Chelyosoma productum
MN138376 Chelyosoma productum
AB104867 Chelyosoma siboja
KY882283 Dicopia fimbriata
AB104866 Megalodicopia hians
MG877561 Corella antarctica
MG877560 Corella antarctica
MG877559 Corella antarctica
KY235545 Corella aff inflata JAM 2017
MH339617 Corella eumyota
KU299765 Corella eumyota
EU140804 Corella eumyota
MG877558 Corella eumyota
AB079784 Ciona savignyi
AJ517314 Ciona robusta
LR216645 Ciona edwardsi
LR217849 Ciona sp n CG 2019
AM292218 Ciona intestinalis
LR216644 Ciona roulei
100/1.0
100/1.0
70/1.0
57/0.98
100/1.0
68/1.0
100/1.0
60/0.74
98/1.0
100/1.0
100/1.0
99/1.0
100/1.0
50/-
97/1.0
95/1.0
100/1.0
80/1.0
78/0.92
91/1.0
95/1.0
89/1.0
97/1.0
96/1.0
99/1.0
100/1.0
72/1.0
100/0.97
84/1.0
100/1.0
100/1.0
91/1.0
100/1.0
100/1.0
-/0.98
-/0.76
100/1.0
100/1.0
73/1.0
100/1.0
100/1.0
51/-
100/1.0
100/1.0
66/0.95
86/1.0
89/1.0
64/0.98
50/-
88/1.0
100/1.0
100/1.0
100/1.0
100/1.0
100/1.0
86/1.0
100/1.0
-/0.76
83/1.0
68/0.97
100/1.0
100/1.0
94/1.0
81/1.0
100/1.0
B
Israel (OX416769)
1
Israel (MW363030)
1
1
2
2
8
19
6
A. malaca (OM912748)
1
A.sydneiensis (MT637975)
1
Israel (OX416774)
1
Israel (OX416767, OX416773)
2
Florida (ON055288)
1
Andaman and Nicobar (KJ725162)
1

◂**Fig. 3** Evolutionary relationships of the obtained *Ascidia virginea* sequences. (**A**) Maximum likelihood tree of phlebobranchian COI sequences. Phylogenetic relationships were inferred from a matrix of 804 nucleotide positions for 141 sequences. Maximum likelihood bootstrap supports above 50% and Bayesian posterior probabilities above 0.75 are indicated near the corresponding node, separated with a slash. Branch supports are not indicated for relationships within a species (short branches). (**B**) Median-joining network of *Ascidia virginea* COI haplotypes (560 bp). Each circle corresponds to a different haplotype, and its size is proportional to the corresponding haplotype frequency. The numbers in the circles indicate haplotype frequencies. The small gray circle indicates a missing intermediate. Tick marks along each branch designate the number of base substitutions between haplotypes. Geographic regions are indicated by different colors (violet: Mediterranean; red: Red Sea; black: Indian Ocean; light blue: NW Atlantic; dark blue: NE Atlantic; green: N Pacific). Distant haplotypes are labeled with their accession number

often leading to high chlorophyll measurements due to algal blooms) is common due to pollution and proximity to urban areas. Indeed, all the *A. virginea* sequences from Florida, California, and Puerto Rico included in our analyses were found in harbors and marinas (Nichols et al. 2023; Nydam unpublished, sequences available in NCBI). Although our model did not indicate that California or Florida are suitable places for *A. virginea*, it is likely that the conditions in the marinas and harbors where the specimens were found are not representative of the conditions in the natural environment of the locations used in the current ENM. Our models revealed that chlorophyll concentration (as a proxy for phytoplankton biomass and for primary production) was one of the major predictors of *A. virginea* distribution, as also reported in previous studies (Lins et al. 2018), and as specifically relevant for cold-water species that are adapted to nutrient-rich environments (Bereza and Shenkar 2022). The current ecological data indicate a lower number of *A. virginea* occurrences in warmer areas (e.g., Levant Basin and the Red Sea) compared to a large number of documented occurrences in cold and temperate areas (e.g., northwestern Atlantic Ocean, Arctic Ocean) (Fig. 1). These data may have biased the habitat suitability results, since the molecular data indicate that this species is already present in Florida and California. Indeed, the ENMs results suggest that the areas where the species is present in Israel are only “moderately suitable” habitats. Although these areas are known to be ultra-oligotrophic with few available nutrients for filter-feeders such as ascidians, solitary ascidians can efficiently capture submicron particles as small as marine bacteria (Jacobi et al. 2018). Thus, ascidians are likely to exploit a large variety of particles as energy sources, which is very significant in niche areas in oligotrophic habitats. However, the diversity of such sources of energy could not be included as a predictor variable in our models due to the lack of available data. Similarly, we could not include precise environmental conditions for the bays and harbors in our ENM analysis, since data from these areas were not available. In particular, we could not add as a predictor variable the presence of artificial habitats, which constitute an important factor and one that is known to facilitate ascidian introductions (Zhang et al. 2020). Furthermore, considering the increased anthropogenic activities in harbors, these areas most likely exhibit higher chlorophyll concentrations that are not reported and could not be considered in the current model. Yet, this may contribute to higher food availability for non-indigenous ascidian species and facilitation of their colonization and establishment.

Indeed, Eilat marina is located in proximity to two international ports: the Port of Aqaba in Jordan and the Port of Eilat in Israel. The increase in maritime activity may contribute to the introduction and spread of non-indigenous marine species in the region, including ascidians such as *A. virginea*, as these organisms can be easily transported as part of the fouling community (Gewing and Shenkar 2017). The close interplay of these ports heightens the potential for species exchange and necessitates vigilant monitoring to manage and mitigate the impact of potentially invasive species on local marine ecosystems (Fernandez et al. 2022).

As previously observed for other ascidian species (e.g., Rocha et al. 2019; Mastrototaro et al. 2019a, 2020b; Montesanto et al. 2021, 2022; Turon et al. 2020; Nichols et al. 2023), the taxonomic identification of *A. virginea* requires detailed analyses, including morphological and molecular tools, since slight differences have been recorded in the morphological features of *A. virginea* specimens, highlighting that the external appearance of this species may vary (i.e., the different distance of the siphons between the specimens collected in the Red Sea and the Eastern Mediterranean Sea). As a case in point, our phylogenetic analysis (Fig. 3) suggests that all our sequences, as well as all public COI sequences assigned to *A.*

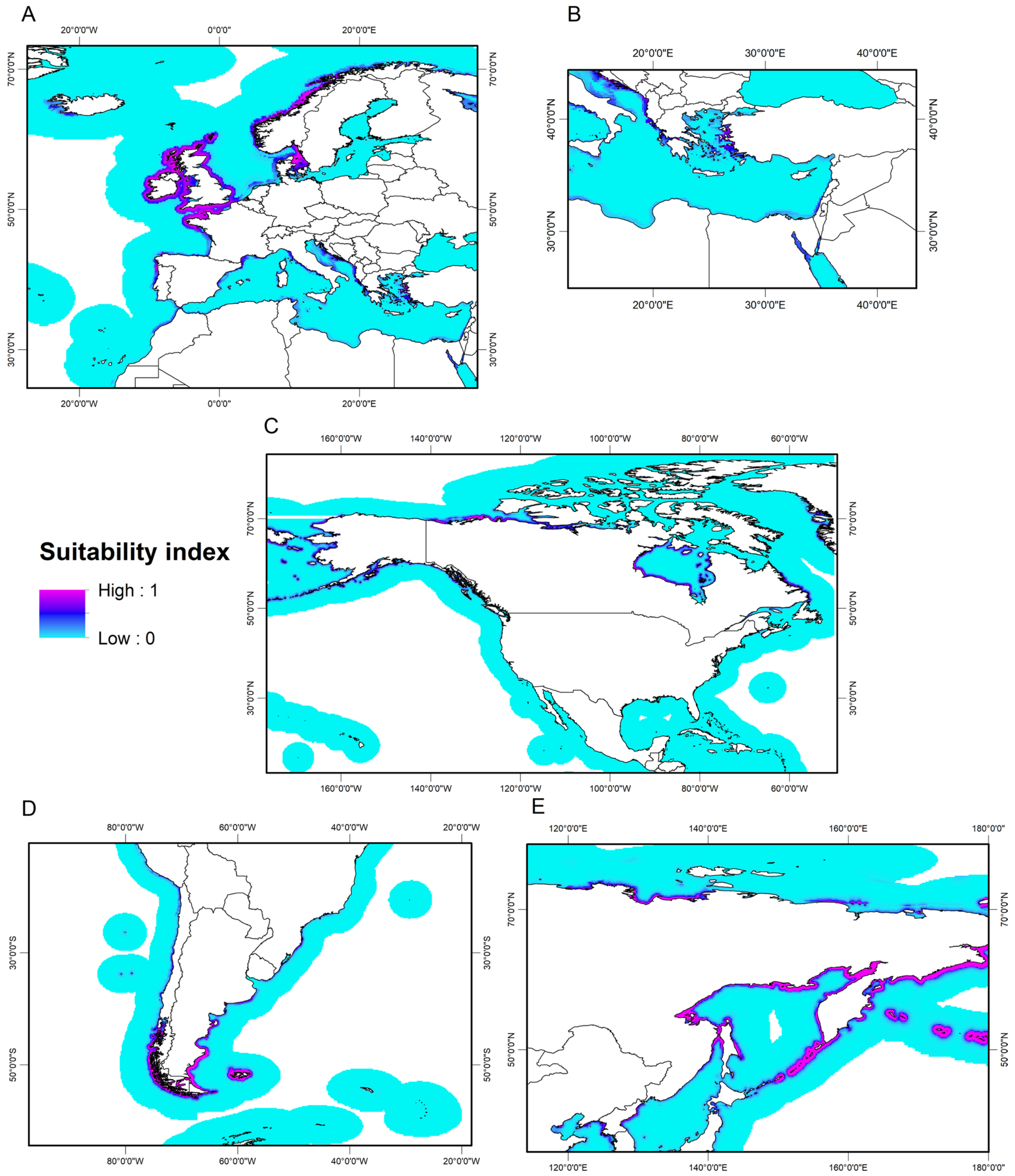

Fig. 4 Projections of the potential distribution of *A. virginea* based on ENM analyses. (**A**) European seas and Red Sea. (**B**) Magnification of the Red Sea area from "European seas and Red Sea" projection. (**C**) North America. (**D**) South America. (**E**) Northwest Pacific Ocean. Purple area represents the highest habitat suitability for *A. virginea*; the light-blue areas represent low suitability areas; and the blue areas represent moderate suitability

malaca (Virgili et al. 2022) and *A. sydneiensis* (Streit et al. 2021), belong to a single species. Moreover, our morphological analyses revealed that all samples investigated in this work should be referred to as *A. virginea* rather than as *A. malaca* or *A. sydneiensis*, due to the position of the siphons. Indeed, the siphons are distant from each other in both *A. malaca* and *A. sydneiensis* (Brunetti and Mastrototaro 2017; Streit et al. 2021; Virgili et al. 2022), while in our specimens they lie closer to each other, they are much shorter compared to the long siphons typical of *A. sydneiensis*, and they lack the strong musculature typical of this latter species (Streit et al. 2021). Regarding the specimens of *A. malaca* described by Virgili et al. (2022), they present a gray-brown leathery external appearance, with a wide gut in the center of the body and ending in a short rectum, with no intermediate papillae on the longitudinal vessels; whereas, our specimens present the gut positioned at the bottom of the body, with a long vertical rectum, and intermediate papillae on longitudinal vessels, which are all typical morphological characters of *A. virginea* (Brunetti and Mastrototaro 2017). The potential synonymy of these three species, suggested by the COI data, could be the result of specimen misidentification or the existence of only slight morphological differences as well as the presence of intra-specific variability that enable the discrimination of one species from another. Consequently, this issue should be further investigated by comparing the original samples analyzed by Streit et al. (2021) and Virgili et al. (2022), as well as by comparing them with the original holotype samples. Further morphological analyses on newly collected samples should be also carried out on specimens originating from the same localities of this study as well as of previous ones (Streit et al. 2021; Virgili et al. 2022), in order to exclude a population-specific morphological variability. Analyses of additional molecular markers (i.e., the entire mitochondrial genome or nuclear genes) are also needed in order to solve this issue. Indeed, Streit et al. (2021) hypothesize that the COI gene of the *Ascidia* genus has evolved at a slower pace, resulting in sequence differences between these species of $< 3\%$. This contrasts the fact that the more divergent *A. virginea* COI sequence KJ725162, from the Indian Ocean (Ananthan and Murugan 2018), shows a 4.5–5.9% divergence from the other conspecific sequences and has the longest branch in Fig. 3A. Moreover, depending on the comparison, this Indian Ocean's more divergent sequence is marginally beyond or above the 5% arbitrary threshold commonly used for species discrimination, further supporting the need to evaluate the variability of this species by using additional molecular markers or at least by increasing the length of the analysed COI fragment. The existence of high sequence divergence at the DNA level but not at the amino acid level (i.e., the amino acid sequence of the specimen from the Indian Ocean's is identical to that of other conspecific specimens) may suggest the presence of high genetic variability between *A. virginea* populations from very distant localities. However, it should be noted that the same authors submitted another *A. virginea* sequence (KP842723), from the same Indian Ocean region, which is identical to our main haplotype (corresponding to accession number ON062302). Because this KP842723 sequence is annotated as "unverified" in the NCBI, it was not included in our NCBI BLAST search and downstream phylogenetic analysis. Nonetheless, it indicates the presence of at least two distant haplotypes of *A. virginea* in the Indian Ocean. Finally, the fact that several haplotypes were found in the western Atlantic suggests that several successful independent introductions have occurred in this region.

Several species of ascidians are known as nuisance species, in their ability to rapidly grow and colonize on any kind of artificial or natural substrate, competing for space and nutrients with the indigenous communities (Lambert 2002, 2007). Recent studies have predicted that species more tolerant to high temperatures, such as *Botrylloides violaceus* Oka, 1927 and *Ciona robusta* (Hoshino and Tokioka 1967), are likely to expand their distribution in warmer areas in the future (Lins et al. 2018). For example, *C. robusta* is already present and established in the Eilat marina (Shenkar et al. 2017), where its presence as yet another non-indigenous species adds a major threat to the nearby fragile coral-reef habitat. Indeed, these opportunistic species, which can tolerate a wide range of environmental parameters, have been shown to be able to outcompete major ecosystem engineers, such as corals, especially in already stressed environments (Roth et al. 2018).

Studies combining morphological and DNA barcoding analyses are a prerequisite for improving the early detection of non-indigenous species, in particular of those organisms that are not easily discriminated by external appearance. Morphological and DNA tools are especially necessary in ports and marinas, since these represent the main gateway for such widely tolerant and opportunistic species characterized by high spread potential. Indeed, since the complete eradication of these species is unlikely, early identification and efficient monitoring surveys are urgently needed in order to enable the establishment of appropriate management strategies to control and prevent the further spread of highly invasive species, particularly in areas where they may represent a potential threat to habitats of immense ecological importance, such as coral reefs.

Acknowledgements We are grateful to the Steinhardt Museum of National History at Tel-Aviv University and the Inter-University Institute (IUI) in Eilat for their technical support, to Michal Haddas-Sasson for her help at the bench and to Naomi Paz for editorial assistance. CG acknowledges the Molecular Biodiversity Laboratory of the Italian node of Lifewatch (CNR, Consiglio Nazionale delle Ricerche, Italy), Elixir-IT (the European Research Infrastructure for Life Science), and CNRBiOmics (Infrastructural project PIR01_00017 of MUR-Ministero dell'Università e della Ricerca, Italy). We wish to thank the editor for his helpful suggestions and acknowledge the anonymous reviewers whose comments considerably improved the manuscript.

Author contributions NS, LN, and FMo collected and preserved the animals. FMo and FMa carried out the morphological analysis. RH, DH, FMo and CG conducted the molecular analysis and RH & DH performed the phylogenetic tree construction, LN and NS took care of the curation, shipment, and specimens' availability. NS and FMo supervised the study and drafted the manuscript together with DH. All authors contributed to the article and approved the submitted version.

Funding FMo was supported by the European Union's Horizon 2020 Research and Innovation program under grant agreement N° 730984, ASSEMBLE Plus project. Additional funding was provided by ISF-NSFC grant number 3347/20 to NS and ISF grant number 652/20 to DH.

Data availability All the uncropped images are available in the Figshare repository (https://doi.org/https://doi.org/10.6084/m9.figshare.22589515 for further images of the dissected specimens). The sequences obtained in this study were deposited to in the European Nucleotide Archive under accession numbers OX416767-OX416775. The sequences are still confidential. The samples examined have been deposited in the Zoological Museum of the University of Bari (MUZAC-6669) and the Steinhardt Museum of Natural History and National Research Center (AS26215-AS26216; AS26223-AS26229; AS26172).

Declarations

Conflict of interest The authors declare that the research was conducted in the absence of any commercial or financial relationships that could be construed as a potential conflict of interest.

References

Adams CM, Shumway SE, Whitlatch RB, Getchis T (2011) Biofouling in marine molluscan shellfish aquaculture: a survey assessing the business and economic implications of mitigation. J World Aquac Soc 42(2):242–252. https://doi.org/10.1111/j.1749-7345.2011.00460.x

Airoldi L, Turon X, Perkol-Finkel S, Rius M (2015) Corridors for aliens but not for natives: effects of marine urban sprawl at a regional scale. Divers Distrib 21(7):755–768. https://doi.org/10.1111/ddi.12301

Aldred N, Clare AS (2014) Mini-review: impact and dynamics of surface fouling by solitary and compound ascidians. Biofouling 30(3):259–270. https://doi.org/10.1080/08927014.2013.866653

Ananthan G, Murugan R (2018) Molecular phylogeny of four ascidian species inferred from mitochondrial Cytochrome Oxidase subunit I (COI) sequence. Mitochondrial DNA A DNA Mapp Seq Anal 29(1):121–125. https://doi.org/10.1080/24701394.2016.1253071

Arnbäck-Christie-Linde A (1923) Northern and arctic invertebrates in the collection of the Swedish State Museum. IX. Tunicata 2:1–25

Assis J, Tyberghein L, Bosch S, Verbruggen H, Serrão EA, De Clerck O (2018) Bio-ORACLE v2.0: extending marine data layers for bioclimatic modelling. Glob Ecol Biogeogr 27:277–284. https://doi.org/10.1111/geb.12693

Bandelt HJ, Forster P, Rohl A (1999) Median-joining networks for inferring intraspecific phylogenies. Mol Biol Evol 16:37–48. https://doi.org/10.1093/oxfordjournals.molbev.a026036

Barve N, Barve V, Jimenez-Valverde A, Lira-Noriega A, Maher SP, Peterson A et al (2011) The crucial role of the accessible area in ecological niche modeling and species distribution modeling. Ecol Model 222:1810–1819. https://doi.org/10.1016/j.ecolmodel.2011.02.011

Basher Z, Bowden DA, Costello MJ (2014) Global marine environment dataset (GMED). Version 1.0 (Rev.01.2014). Available from: http://gmed.auckland.ac.nz

Bay-Nouailhat A, Bay-Nouailhat W (2020) Guide des Tuniciers de l'Europe de l'Ouest. M&L Éditions

Belmonte G, Potenza D (2001) Biogeography of the family Acartiidae (Calanoida) in the Ponto-Mediterranean province. Hydrobiologia 453:171–176

Bereza D, Shenkar N (2022) Shipping voyage simulation reveals abiotic barriers to marine bioinvasions. Sci Total Environ 837:155741

Berrill NJ (1950) The Tunicata with an account of the British species. Ray Society

Brunetti R, Mastrototaro F (2017) Ascidiacea of the European waters. Edagricole–New Business Media II, Milan

Carlos-Júnior LA, Barbosa NPU, Moulton TP, Creed JC (2015) Ecological Niche Model used to examine the distribution of an invasive, non-indigenous coral. Mar Environ Res 103:115–124. https://doi.org/10.1016/j.marenvres.2014.10.004

Casso M, Navarro M, Ordóñez V, Fernández-Tejedor M, Pascual M, Turon X (2018) Seasonal patterns of settlement and growth of introduced and native ascidians in bivalve cultures in the Ebro Delta (NE Iberian Peninsula). Reg

Stud Mar Sci 23:12–22. https://doi.org/10.1016/j.rsma.2017.11.002

Cassini MH (2011) Ecological principles of species distribution models: the habitat matching rule. J Biogeogr 38:2057–2065. https://doi.org/10.1111/j.1365-2699.2011.02552.x

Chang AL, Carlton JT, Brown CW, Ruiz GM (2020) Down the up staircase: equatorward march of a cold-water ascidian and broader implications for invasion ecology. Divers Distrib 26(7):881–896. https://doi.org/10.1111/ddi.13055

Dormann CF, Elith J, Bacher S, Buchmann C, Carl G, Carré G et al (2013) Collinearity: a review of methods to deal with it and a simulation study evaluating their performance. Ecography 36:27–46. https://doi.org/10.1111/j.1600-0587.2012.07348.x

Fernandez S, Ardura A, Georges O, Martinez JL, Suarez-Menendez M, Planes S, Garcia-Vazquez E (2022) Non-native species in the north Gulf of Aqaba (Red Sea) revealed from environmental DNA. Front Mar Sci 9:940889

Franklin J (2010) Mapping species distributions: spatial inference and prediction. Cambridge University Press, Cambridge

Fulton TM, Chunwongse J, Tanksley SD (1995) Microprep protocol for extraction of DNA from tomato and other herbaceous plants. Plant Mol Biol Rep 13:207–209. https://doi.org/10.1007/BF02670897

Gewing MT, Shenkar N (2017) Monitoring the magnitude of marine vessel infestation by non-indigenous ascidians in the Mediterranean. Mar Pollut Bull 121(1–2):52–59. https://doi.org/10.1016/j.marpolbul.2017.05.041

Ghobashy AFA, Abdel Messeih MK (1991) Ascidians in Egyptian waters. J Egypt German Soc Zool 4:313–326

Heller C (1875) Untersuchungen über die Tunicaten des Adriatischen Meeres. Denkschriften der Kaiserlichen Academie der Wissenschaften. Mathematisch-Naturwissenschaftliche Classe, Wien

Jacobi Y, Yahel G, Shenkar N (2018) Efficient filtration of micron and submicron particles by ascidians from oligotrophic waters. Limnol Oceanogr 63(S1):S267–S279. https://doi.org/10.1002/lno.10736

Januario SM, Estay SA, Labra FA, Lima M (2015) Combining environmental suitability and population abundances to evaluate the invasive potential of the tunicate *Ciona intestinalis* along the temperate South American coast. PeerJ 3:e1357. https://doi.org/10.7717/peerj.1357

Katoh K, Standley DM (2013) MAFFT Multiple Sequence Alignment Software Version 7: improvements in performance and usability. Mol Biol Evol 30(4):772–780. https://doi.org/10.1093/molbev/mst010

Koukouras A, Voultsiadou-Koukoura E, Kevrekidis T, Vafidis D (1995) Ascidian fauna of the Aegean Sea with a check list of the eastern Mediterranean and Black Sea species. In: Annales de l'Institut océanographique, vol 71. Impr. de Monaco 1909–2002, Monaco, pp 19–34

Lambert G (2002) Non-indigenous ascidians in tropical waters. Pac Sci 56(3):291–298

Lambert G (2007) Invasive sea squirts: a growing global problem. J Exp Mar Biol Ecol 342(1):3–4. https://doi.org/10.1016/J.JEMBE.2006.10.009

Lima FP, Ribeiro PA, Queiroz N, Hawkins SJ, Santos AM (2007) Do distributional shifts of northern and southern species of algae match the warming pattern? Glob Change Biol 13(12):2592–2604

Lins DM, de Marco P, Andrade AF, Rocha RM (2018) Predicting global ascidian invasions. Divers Distrib 24(5):692–704. https://doi.org/10.1111/ddi.12711

Liu X, Guo Z, Ke Z, Wang S, Li Y (2011) Increasing potential risk of a global aquatic invader in Europe in contrast to other continents under future climate change. PLoS ONE 6(3):e18429. https://doi.org/10.1371/journal.pone.0018429

Locke A, Hanson JM (2009) Rapid response to non-indigenous species. 1. Goals and history of rapid response in the marine environment. Aquat Invasion 4(1):237–247. https://doi.org/10.3391/ai.2009.4.1.24

López-Legentil S, Legentil ML, Erwin PM, Turon X (2015) Harbor networks as introduction gateways: contrasting distribution patterns of native and introduced ascidians. Biol Invasions 17(6):1623–1638. https://doi.org/10.1007/s10530-014-0821-z

Malaquias MA, Zamora-Silva A, Vitale D, Spinelli A, De Matteo S, Giacobbe S et al (2016) The Mediterranean Sea as a gateway for invasion of the Red Sea: the case of the Indo-West Pacific head-shield slug *Chelidonura fulvipunctata* Baba, 1938. Aquat Invasion 11:247–255. https://doi.org/10.3391/ai.2016.11.3.03

Mastrototaro F, Montesanto F (2022) The new checklist of the Italian fauna: Ascidiacea. Biogeogr. J. Integr. Biogeogr. 37(1):200. https://doi.org/10.21426/B637156606

Mastrototaro F, Montesanto F, Salonna M, Grieco F, Trainito E, Chimienti G et al (2019a) Hitch-hikers of the sea: concurrent morphological and molecular identification of *Symplegma brakenhielmi* (Tunicata: Ascidiacea) in the western Mediterranean Sea. Med Mar Sci 20:197–207. https://doi.org/10.12681/mms.19390

Mastrototaro F, Chimienti G, Montesanto F, Perry AL, García S, Alvarez J et al (2019b) Finding of the macrophagous deep-sea ascidian *Dicopia antirrhinum* Monniot, 1972 (Chordata: Tunicata) in the Tyrrhenian Sea and updating of its distribution. Eur Zool J 86(1):181–188. https://doi.org/10.1080/24750263.2019.1616838

Mastrototaro F, Aguilar R, Alvarez H, Blanco J, García S, Montesanto F et al (2020a) Mesophotic rocks dominated by *Diazona violacea*: a Mediterranean codified habitat. Eur Zool J 87(1):688–695. https://doi.org/10.1080/24750263.2020.1837972

Mastrototaro F, Montesanto F, Salonna M, Viard F, Chimienti G, Trainito E et al (2020b) An integrative taxonomic framework for the study of the genus *Ciona* (Ascidiacea) and description of a new species, *Ciona intermedia*. Zool J Linn Soc 190(4):1193–1216. https://doi.org/10.1093/zoolinnean/zlaa042

Mastrototaro F, Gasparini F, Montesanto F (2022) The clubbed tunicate *Styela clava* has arrived in the Lagoon of Venice. Eur Zool J 89(1):502–509. https://doi.org/10.1080/24750263.2022.2052989

Melo-Merino SM, Reyes-Bonilla H, Lira-Noriega A (2020) Ecological niche models and species distribution models in marine environments: a literature review and spatial analysis of evidence. Ecol Model 415:108837

Millar RH (1966) Tunicata Ascidiacea. Marine Invertebrates of Scandinavia, Oslo

Millar RH (1970) British Ascidians. Linnean Society of London by Academic Press, London and New York

Montesanto F, Chimienti G, Gissi C, Mastrototaro F (2021) Spread of the non-indigenous ascidian *Aplidium accarense* (Millar, 1953) in the Eastern Mediterranean Sea: morphological and molecular tools for an accurate identification. Med Mar Sci 22(2):246–254. https://doi.org/10.12681/mms.24887

Montesanto F, Chimienti G, Gissi C, Mastrototaro F (2022) *Polyclinum constellatum* (Tunicata, Ascidiacea), an emerging non-indigenous species of the Mediterranean Sea: integrated taxonomy and the importance of reliable DNA barcode data. Med Mar Sci 23(1):69–83. https://doi.org/10.12681/mms.28311

Müller OF (1776) Zoologiæ Danicæ Prodromus, seu Animalium Daniæ et Norvegiæ indigenarum characteres, nomina, et synonyma imprimis popularium. Havniæ [Copenhagen], Hallageri, p 274

Nguyen L-T, Schmidt HA, von Haeseler A, Minh BQ (2015) IQ-TREE: a fast and effective stochastic algorithm for estimating maximum likelihood phylogenies. Mol Biol Evol 32:268–274. https://doi.org/10.1093/molbev/msu300

Nichols CL, Lambert G, Nydam ML (2023) Continued persistence of non-native ascidians in Southern California harbors and marinas. Aquat Invasions 18:1–22

Nydam ML, Nichols CL, Lambert G (2022) First record of the ascidian *Ascidiella aspersa* (Müller, 1776) in southern California. BioInvasions Rec 11(2):416–427

Nye JA, Link JS, Hare JA, Overholtz WJ (2009) Changing spatial distribution of fish stocks in relation to climate and population size on the Northeast United States continental shelf. Mar Ecol Prog Ser 393:111–129. https://doi.org/10.3354/meps08220

Owens HL, Campbell LP, Dornak LL, Saupe EE, Barve N, Soberón J et al (2013) Constraints on interpretation of ecological niche models by limited environmental ranges on calibration areas. Ecol Model 263:10–18. https://doi.org/10.1016/j.ecolmodel.2013.04.011

Paithankar KR, Prasad KS (1991) Precipitation of DNA by polyethylene glycol and ethanol. Nucleic Acids Res 19(6):1346. https://doi.org/10.1093/nar/19.6.1346

Pearson RG (2007) Species Distribution Modeling for conservation educators and practitioners. Lessons Conserv 3:54–89

Pérès JM (1957) Ascidies récoltées dans les parages des Baléares par le 'Professeur Lacaze-Duthiers'(2e. partie): Iviza et San Antonio. Vie Milieu 6:223–234

Peterson AT (2011) Ecological niche conservatism: a time-structured review of evidence. J Biogeogr 38:817–827. https://doi.org/10.1111/j.1365-2699.2010.02456.x

Phillips SJ, Anderson RP, Schapire RE (2006) Maximum entropy modeling of species geographic distributions. Ecol Model 190:231–259. https://doi.org/10.1016/j.ecolmodel.2005.03.026

Petović S, Grieco F, Macic V, Montesanto F, Mastrototaro F (2018) New data *on Aplidium tabarquense* (Tunicata: Ascidiacea) distribution in the Adriatic Sea. Turk J Zool 42(1):146–151. https://doi.org/10.3906/zoo-1705-49

Phillips, S.J., Dudík, M., and Schapire, R.E. (2004). A maximum entropy approach to species distribution modeling. In: Twenty-first international conference on machine learning ICML'04. ACM Press, New York, p 83

Pinsky ML, Worm B, Fogarty MJ, Sarmiento JL, Levin SA (2013) Marine taxa track local climate velocities. Science 341(6151):1239–1242. https://doi.org/10.1126/science.123935

Pinsky ML, Selden RL, Kitchel ZJ (2020) Climate-driven shifts in marine species ranges: scaling from organisms to communities. Ann Rev Mar Sci 12:153–179. https://doi.org/10.1146/annurev-marine-010419-010916

Rocha RC, Monnington JM, Newstead RG, Sambrook K, Griffith K, Holt RHF et al (2015) Recreational vessels as a vector for marine non-natives: developing biosecurity measures and managing risk through an in-water encapsulation system. Hydrobiologia 750:187–199

Rocha RM, Salonna M, Griggio F, Ekins M, Lambert G, Mastrototaro F et al (2019) The power of combined molecular and morphological analyses for the genus *Botrylloides*: identification of a potentially global invasive ascidian and description of a new species. Syst Biodivers 17(5):509–526. https://doi.org/10.1080/14772000.2019.1649738

Ronquist F, Teslenko M, van der Mark P, Ayres DL, Darling A, Höhna S, Larget B et al (2012) MRBAYES 3.2: efficient Bayesian phylogenetic inference and model selection across a large model space. Syst Biol 61:539–542. https://doi.org/10.1093/sysbio/sys029

Roth SK, Powell A, Smith DJ, Roth F, Schierwater B (2018) The highly competitive ascidian *Didemnum* sp. threatens coral reef communities in the Wakatobi Marine National Park, Southeast Sulawesi, Indonesia. Reg Stud Mar Sci 24:48–54. https://doi.org/10.1016/j.rsma.2018.07.001

Salfi M (1931) Gli ascidiacei del Golfo di Napoli. Pubbl Della Stn Zool Napoli 11:293–360

Salonna M, Gasparini F, Huchon D, Montesanto F, Haddas- Sasson M, Ekins M et al (2021) An elongated COI fragment to discriminate botryllid species and as an improved ascidian DNA barcode. Sci Rep 11(1):1–19. https://doi.org/10.1038/s41598-021-83127-x

Seebens H, Gastner MT, Blasius B (2013) The risk of marine bioinvasion caused by global shipping. Ecol Lett 16:782–790. https://doi.org/10.1111/ele.12111

Shenkar N (2012) Ascidian (Chordata, Ascidiacea) diversity in the Red Sea. Mar Biodivers 42(4):459–469. https://doi.org/10.1007/s12526-012-0124-5

Shenkar N, Swalla BJ (2011) Global diversity of Ascidiacea. PLoS ONE 6(6):e20657. https://doi.org/10.1371/journal.pone.0020657

Shenkar N, Koplovitz G, Dray L, Gissi C, Huchon D (2016) Back to solitude: solving the phylogenetic position of the Diazonidae using molecular and developmental characters. Mol Phylogenet Evol 100:51–56. https://doi.org/10.1016/j.ympev.2016.04.001

Shenkar N, Shmuel Y, Huchon D (2017) The invasive ascidian *Ciona robusta* recorded from a Red Sea marina. Mar Biodivers 48(4):2211–2214. https://doi.org/10.1007/s12526-017-0699-y

Skinner LF, Barboza DF, Rocha RM (2016) Rapid Assessment Survey of introduced ascidians in a region with many marinas in the southwest Atlantic Ocean. Braz Manag Biol Invas 7(1):13–20. https://doi.org/10.3391/mbi.2016.7.1.03

Simkanin C, Davidson IC, Dower JF, Jamieson G, Therriault TW (2012) Anthropogenic structures and the infiltration of natural benthos by invasive ascidians. Mar Ecol 33(4):499–511. https://doi.org/10.1111/j.1439-0485.2012.00516.x

Stachowicz JJ, Terwin JR, Whitlatch RB, Osman RW (2002) Linking climate change and biological invasions: ocean warming facilitates nonindigenous species invasions. Proc Natl Acad Sci 99(24):15497–15500. https://doi.org/10.1073/pnas.242437499

Stamatakis A (2014) RAxML version 8: a tool for phylogenetic analysis and post-analysis of large phylogenies. Bioinformatics 30(9):1312–1313. https://doi.org/10.1093/bioinformatics/btu033

Streit OT, Lambert G, Erwin PM, López-Legentil S (2021) Diversity and abundance of native and non-native ascidians in Puerto Rican harbors and marinas. Mar Pollut Bull 167:112262. https://doi.org/10.1016/j.marpolbul.2021.112262

Swets JA (1988) Measuring the accuracy of diagnostic systems. Science 240:1285–1293. https://doi.org/10.1126/science.3287615

Tiralongo F, Messina G, Lombardo BM (2021) Invasive species control: predation on the alien crab *Percnon gibbesi* (H. Milne Edwards, 1853) (Malacostraca: Percnidae) by the rock goby, *Gobius paganellus* Linnaeus, 1758 (Actinopterygii: Gobiidae). J Mar Sci Eng 9(4):393. https://doi.org/10.3390/jmse9040393

Traustedt MPA (1883) Die einfachen Ascidien des Golfes von Neapel. Mitth Zool Stat Neapel 4:448

Turon X, Casso M, Pascual M, Viard F (2020) Looks can be deceiving: *Didemnum pseudovexillum* sp. Nov. (Ascidiacea) in European harbours. Mar Biodivers 50(4):1–14. https://doi.org/10.1007/s12526-020-01083-7

VanDerWal J, Shoo LP, Graham C, Williams SE (2009) Selecting pseudo-absence data for presence-only distribution modeling: how far should you stray from what you know? Ecol Model 220:589–594. https://doi.org/10.1016/j.ecolmodel.2008.11.010

Virgili R, Tanduo V, Katsanevakis S, Terlizzi F, Villani G, Fontana A et al (2022) The Miseno Lake (central-western Mediterranean Sea): an overlooked reservoir of non-indigenous and cryptogenic ascidians in a marine reserve. Front Mar Sci 9:866906. https://doi.org/10.3389/fmars.2022.866906

Zhan A, Briski E, Bock DG, Ghabooli S, MacIsaac HJ (2015) Ascidians as models for studying invasion success. Mar Biol 162(12):2449–2470. https://doi.org/10.1007/s00227-015-2734-5

Zhang Z, Capinha C, Karger DN, Turon X, MacIsaac HJ, Zhan A (2020) Impacts of climate change on geographical distributions of invasive ascidians. Mar Environ Res 159:104993. https://doi.org/10.1016/j.marenvres.2020.104993